Flexibility of Monomeric and Dimeric HIV-1 Protease†

Yaakov Levy*,‡,§ and Amedeo Caflisch*,||

Department of Chemical Physics, School of Chemistry, Tel Aviv University, Tel Aviv 69978, Israel, and Department of Biochemistry, University of Zurich, Winterthurerstrasse 190, CH-8057 Zurich, Switzerland

Received: September 5, 2002; In Final Form: December 12, 2002

The flexibility and stability of both monomeric and dimeric HIV-1 PR were explored by 100 ns implicit solvent molecular dynamics simulation at 350 K with the aim to correlate the monomer stability with the dimerization mechanism. The principal component analysis (PCA) was applied to visualize the available regions in the conformational space of the two HIV-1 PR forms, to compare their structural diversity and to map the bottom of their underlying energy landscapes. It was found that whereas the flap tips (residues 45−55) are flexible and adopt close and open conformations in both monomeric and dimeric forms, the N- and C-termini (residues 1−4 and 96−99, respectively), which constitute the interface between the two subunits, are flexible only in the monomer. The different flexibility of the monomeric and dimeric HIV-1 PR is reflected in the different topography of their underlying energy landscape. Although the bottom of the monomer energy landscape is broad and rough, that of the dimer is narrower, deeper, and smoother, reflecting the enhanced flexibility of the monomer and the stabilizing interactions between the dimer subunits. Accordingly, blocking one or both terminals may prevent the formation of the active site. Despite the different flexibility of the termini in the monomeric and dimeric HIV-1 PR, their secondary structure contents are similar. The partial stability of the monomer together with the flexibility of its termini suggest that the HIV-1 PR is not a two-state dimer, as indicated by equilibrium denaturation experiments, but a three-state dimer with a marginally stable monomeric intermediate. This involves the swapping of the flexible termini across the two chains to form the dimer interface.

Introduction

Many proteins carry out their biological function as multimeric assemblies.[1] Though small monomeric proteins are essential for rapid diffusion to the sites of action and for stability at low concentration, larger oligomeric proteins are more stable against denaturation, have a reduced surface area, and can involve a cooperative interaction between the subunits. In particular, homooligomers are favored because the association of several small individual subunits allows the creation of a large structure with a minimum of genetic material. Homo-oligomers are advantageous not only with respect to coding efficiency but also because their construction involves an error control, as a single point error may be reduced more easily by discarding the defected subunit. The formation of macromolecular structures from identical components is frequently associated with high symmetry.[2] The advantage of symmetrical complexes over asymmetric aggregates in the evolution of oligomeric proteins is due to the stability of the association, which is a consequence of the specificity of protein−protein interfaces and the maximum numbers of intersubunit interactions. It has been suggested that a symmetrical protein structure is not only favorable thermodynamically but also kinetically as its energy landscape is smoother and thus includes fewer kinetics barriers to folding than that of completely asymmetric structures.[3] Moreover, the point group symmetry provides a method to create oligomers of defined copy number and thus avoids aggregation, which is associated with diseases such as sickle-cell anemia, Alzheimer's disease, and prion-related diseases.[4−6]

Although the chemical and biological advantages of a symmetric oligomeric protein in comparison to a monomeric protein are familiar, the mechanism and evolutionary pathway of their formation is still under study.[7−9] Recently, Nussinov and her colleagues[7] classified the symmetric homodimers into three groups according to the mechanism of their association: 2-state and 3-state association and domain swapping mechanism. The 2-state model suggests that folded dimers (N_2) are in equilibrium with unfolded monomers (U) and that individual folded monomers (N) do not exist.

$$N_2 \leftrightarrow 2U \tag{1}$$

The dissociation equilibrium constant, K_d, for 2-state dimers is often measured with denaturation equilibrium experiments.[10−12] In the 3-state model the formation of a stable monomer, which is detected experimentally as an intermediate state, is a prerequisite for the association.

$$N_2 \overset{K_1}{\longleftrightarrow} 2N \overset{K_2}{\longleftrightarrow} 2U \tag{2}$$

$$K_1 = [N]^2/[N_2] \qquad K_2 = [U]/[N] \tag{3}$$

Because the overall equilibrium constant for unfolding, K_u ($=K_1K_2^2$), depends on the two coupled equilibrium constants, the unfolding of a three-state dimer is expected to be concentra-

† Abbreviations: HIV-1, human immunodeficiency virus type 1; PR, protease; PCA, principal component analysis; RMSD, root-mean-square deviation; MD, molecular dynamics.

‡ Tel Aviv University.

§ Current address: Department of Chemistry and Physics, University of California at San Diego, 9500 Gilman drive, La Jolla, CA 92093-0371.

|| University of Zurich.

10.1021/jp0219956 CCC: $25.00
Published on Web 03/12/2003

tion dependent.[13] One should note that for $K_2 \gg K_1$ eq 2 represents a two-state dimer. For some three-state homodimeric proteins, a dimeric intermediate is detected rather than a monomeric one; however, this type of dimer is not discussed here. The domain swapping mechanism[14−16] is characterized by replacing one segment in a monomer by an equivalent segment from an identical chain in the dimer. A domain swapped dimer can fold via a two-state mechanism or via a three-state mechanism where a partially stable monomer constitutes the intermediate state. Understanding the mechanism of dimerization is important not only for the origin of oligomers but also for the design of functional oligomers. Moreover, the mechanism by which an unstable monomer forms a stable functional homodimer is important for the understanding of binding and recognition processes. Recently, an increasing body of experimental evidence indicates that for certain proteins folding and binding to small ligands are coupled processes, similar to a two-state dimerization, and that the unbound protein is intrinsically unstructured.[17−19]

In the present study, the effect of dimerization on the flexibility and stability is explored using molecular dynamics (MD) simulations with the aim to correlate the monomer stability with the dimerization mechanism. To address these issues, we selected the homodimeric human immunodeficiency virus type 1 (HIV-1) protease (PR), a dimer with a key role in maturation and replication of the virus that causes the acquired immunodeficiency syndrome (AIDS). The HIV-1 PR is a homodimer with C_2 symmetry in the absence of ligands[20,21] that has been intensively studied both theoretically and experimentally. The enzyme is an aspartic protease that consists of two identical 99 residue subunits, each containing one catalytic aspartic acid (Asp25). The active site region is capped by two identical β-hairpin loops, the flaps, residues 45−55 in each monomer (Figure 1a), which regulate substrate entry into the active site. Although the flap β-hairpins in the ligand-bound protease are well-ordered and interact with the substrate, in the free protease the flaps are very flexible and adopt close and open conformations.[22−26] The two subunits are stabilized by intermolecular interactions, and the largest part of the interface is formed by a four-stranded antiparallel β-sheet consisting of the N- and C-termini of the protease monomers (residues 1−4 and 96−99, respectively, Figure 1b). Two main strategies are used to develop inhibitors for the HIV-1 PR: designing inhibitors that compete with natural substrates for the same active site[27−30] or, alternatively, developing compounds that destabilize the dimeric structure of the protease by binding at the subunit interface.[31−33] Because the active site is defined by the two subunits and does not exist in a single monomer, disruption or destabilization of the dimer will therefore destroy its activity. The design of more powerful dissociative inhibitors will be facilitated by an accurate knowledge of the dimerization energetics and the structural stability of the dimer as well as of the isolated monomer.

The flexibility and stability of both monomeric and dimeric HIV-1 PR are studied by sampling their conformational spaces from 100 ns MD simulation at 350 K using an implicit solvent model. The relatively high value of the temperature was chosen to improve sampling of conformational space. Experimental data on an HIV-1 PR mutant indicate that the monomeric structure is essentially identical to a single subunit of the dimer.[34] The principal component analysis (PCA) was applied to visualize the available regions of the conformational space, to compare their structural diversity, and to map the bottom of their underlying energy landscapes. MD simulations were previously

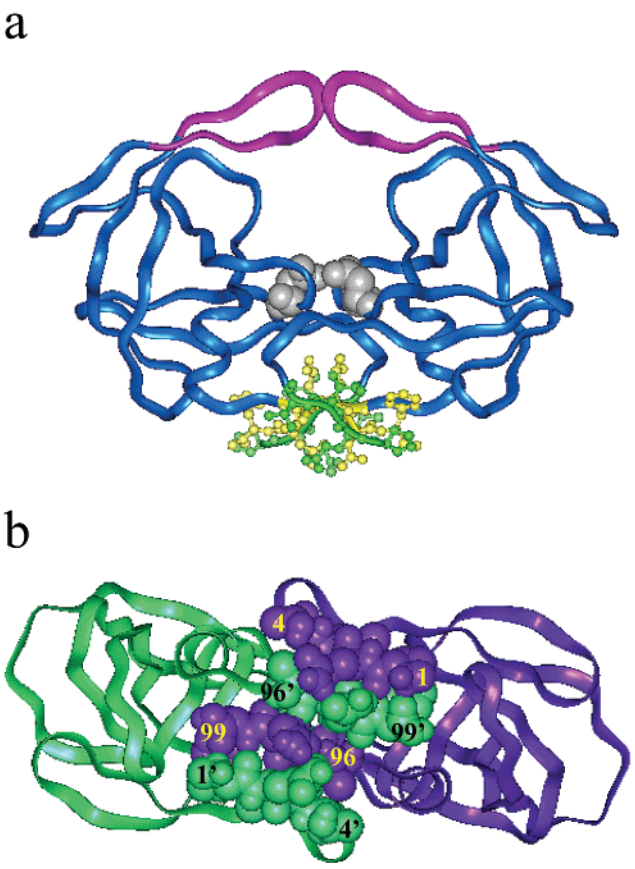

Figure 1. Two orientations of the HIV-1 protease homodimer showing the active site of the enzyme and the interface between the two subunits. (a) The active site is defined by Asp25 of the two subunits (represented by gray vdW spheres). The flap tips (residues 45−55) of each subunit that allow substrate entry to the active site are represented by pink ribbon. The N- and C-termini (residues 1−4 and 96−99) are shown by green and yellow ball-and-stick representation, respectively. (b) The two subunits were colored by different colors, and the four-stranded antiparallel β-sheet is represented by spheres. The interface of the two subunits illustrate a domain swapping mechanism, which involve the exchange of the termini across the two chains.

used to study the dynamics of both monomeric[35] and dimeric[25,36−40] forms of HIV-1 PR. Although the flaps were found to be very flexible in the dimeric form, in agreement with experimental studies,[22,24,26] the N- and C-termini that constitute the interface between the two subunits were found to be flexible only in the monomeric form. However, based on these MD studies, a comparison between the flexibility of the two forms might be misleading due to different time scales. Although the longest simulation of the dimer sampled 10 ns, the isolated monomer was simulated for only 160 ps. Additional regions of the monomeric protein might be flexible (e.g., secondary structure elements) on longer time scales. Moreover, experimental denaturation studies classified HIV-1 PR as a two-state dimer where the dissociation of the dimer and its unfolding are concomitant processes and the monomer is unstructured in solution.[12,41,42] Accordingly, longer MD simulations of the isolated HIV-1 PR monomer are required to study its flexibility and to specifically address the question of the coupling of dissociation with unfolding and between assembling with folding.

Methods

The flexibility of monomeric and dimeric HIV-1 PR was studied by molecular dynamic simulations at 350 K. The initial

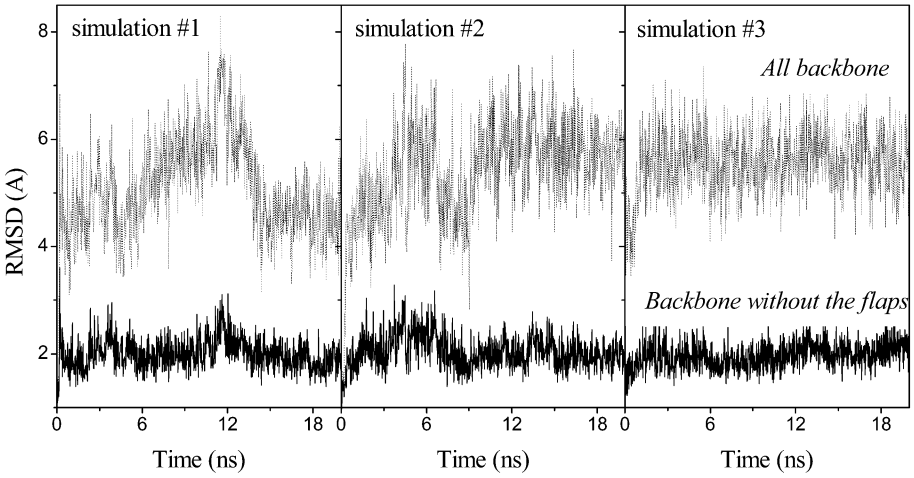

Figure 2. Average RMS deviation of the HIV-1 PR along three 300 K molecular dynamics trajectories relative to the PDB structure. The RMS deviations are based on all backbone atoms (thin line) and backbone atoms excluding the flap regions (thick line). The RMS values indicate that most of HIV-1 PR is stable and that the pronounced flexibility of the dimeric HIV-1 PR at 300 K is due to the flap regions.

conformation in the simulations of the dimeric molecule was the crystal structure of the unliganded protease (PDB entry 1hhp[43]) and the conformation of the monomeric molecule was a single subunit of the homodimer. For each system (monomeric or dimeric HIV-1 PR), five trajectories (each of 20 ns) were performed. Conformations were sampled every 20 ps along the trajectories, resulting in a total of 5000 conformations of monomeric and dimeric HIV-1 PR. The two conformational samples were reduced by applying a distance criterion for similar conformations. Two monomeric/dimeric conformations are defined as being similar if the all-atom Cartesian rms deviation between the conformations is smaller than 2.0/1.8 Å, respectively. After the redundant conformations were removed, the diluted samples included 1512 distinct monomeric HIV-1 PR and 1210 distinct dimeric HIV-1 PR. All simulations were performed with the molecular dynamics program CHARMM[44] and the param19 polar hydrogen force field[44] using 2 fs time steps and a 10 Å cutoff for the nonbonding interactions.

The simulations were performed with the EEF1 implicit solvent model,[45] which approximates the solvation-free energy as a sum over group contributions, where the solvation-free energy of each group is corrected for the screening by surrounding groups in the first solvation shell. This model uses neutralized ionic side chains and a linear distance-dependent dielectric function to simulate the shielding effects of water on electrostatic interaction. The EEF1 model has been shown to give good results for the folding[46−48] and unfolding[49,50] processes of various proteins and is able to discriminate between native and misfolded protein structures.[51−53] Moreover, simulations using this model have been shown to yield a good agreement with explicit solvent simulations.[45,54−56]

To examine the stability of the dimeric HIV-1 protease with the EEF1 force field, three 20 ns MD simulations of the dimer were performed at 300 K. The three trajectories differ in the value of the seed used for generating the random numbers that assign the initial velocities. The structural stability along these trajectories is evaluated by the root-mean-square deviation (RMSD) relative to the X-ray structure after least square superposition. The RMS deviation d_{ij} between conformation i and j of a given molecule is defined as the minimum of the functional

$$d_{ij} = \sqrt{\frac{1}{N}\sum_{k=1}^{N} |r_k^{(i)} - r_k^{(j)}|^2} \qquad (4)$$

where N is the number of atoms in the summation, k is an index over these atoms, and $r_k^{(i)}$, $r_k^{(j)}$ are the Cartesian coordinates of atom k in conformation i and j. Because several experimental and theoretical studies indicated that the flap tips (residues 45−55 of each dimer subunit, see Figure 1) are flexible in solution, the RMSD was calculated on the basis of backbone atoms, both including and excluding the flap residues. The average RMS deviations with and without the flap regions are 5.3 and 2.0 Å, respectively (Figure 2). This indicates that the HIV-1 PR dimer is stable and that the pronounced flexibility at 300 K is located in the flap regions.

To estimate and compare the flexibility of monomeric and dimeric HIV-1 PR, the principal component analysis (PCA)[57−62] was applied on a distance matrix to project the high-dimensional molecular conformational spaces of monomeric and dimeric HIV-1 PR onto a low dimensional sub-space. A distance matrix based PCA was applied in this study, although it is computationally more expensive than the more common covariance matrix based PCA. Though the latter concentrates on the collective motion of the atoms and was successfully applied to find functionally relevant motions,[57−60,62,63] the distance-matrix based PCA concentrates on the structural diversity in conformational samples. Recently, the distance-based PCA has been used to compare the conformational spaces of analogous molecules and in that way has provided a visualization and a quantitative measure for the shifting and shrinking of the conformational space as a result of structural constraints,[64] point mutations,[56,65] and the chemical environment.[55] The distance matrix based PCA was applied here to visualize the effect of dimerization on the flexibility of HIV-1 PR and to quantify the different conformational space of its monomer and dimer.

A key element in the distance matrix based PCA is the choice of distance measure used to construct the distance matrix Δ, which reflects the relationship between the conformations. In this study, the distance between any pair of conformations is measured as the RMS deviation in Cartesian coordinates (eq 4). The minimum value of eq 4 is obtained by an optimal superposition of the two structures. The resulting RMS deviations are usually compiled into an upper diagonal distance matrix Δ_a, where the elements Δ_{ij} are the RMSD between conformations i and j of molecule a (for $i > j$). When conformations of two analogous molecules a and b (or of different samples of the same molecule) are to be compared with each other, the "cross"-distance matrix, $\Delta_{a,b}$, must be calculated in addition to

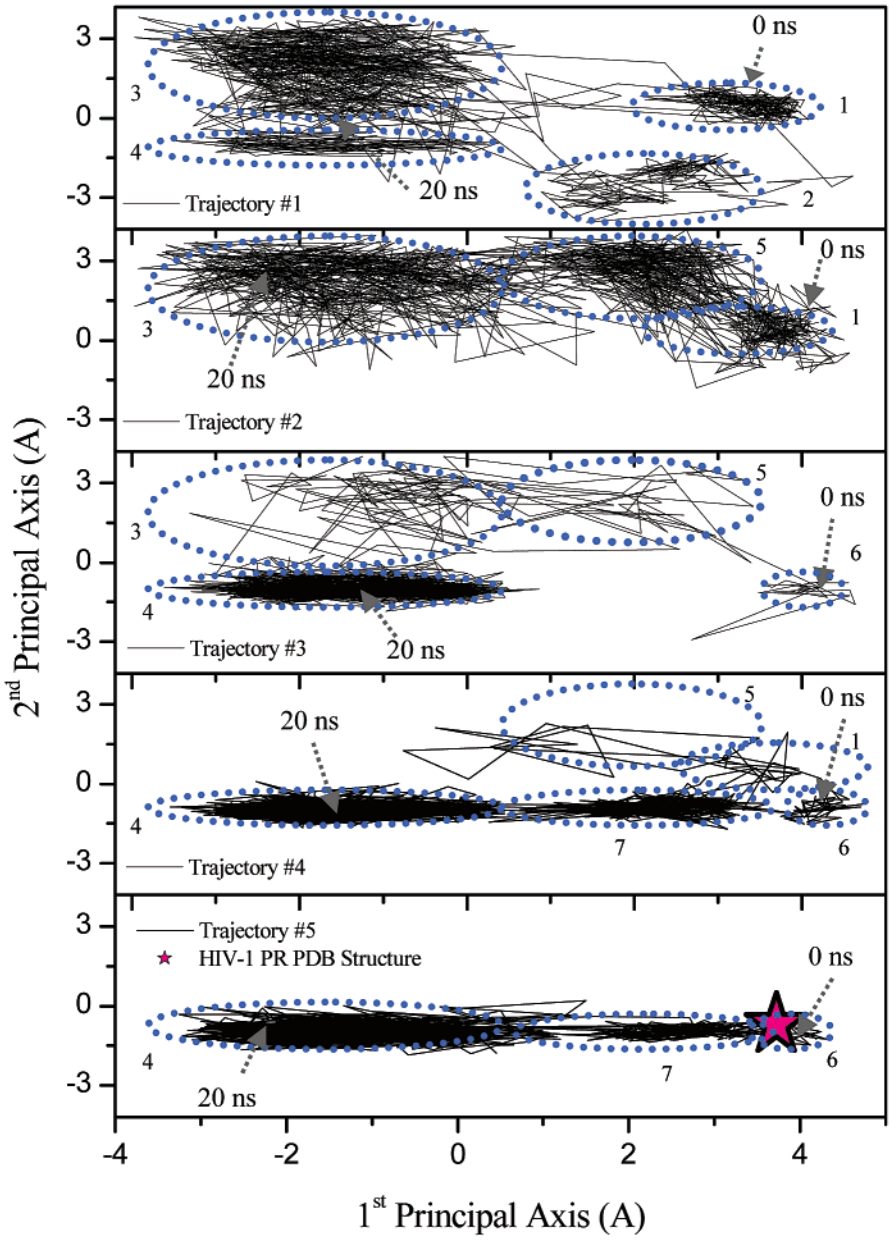

Figure 3. Projections of the five trajectories (simulated at 350 K) of monomeric HIV-1 PR onto a plane defined by the first two principal coordinates. Each trajectory includes 1000 conformations sampled along 20 ns. The initial and final sampled conformations in each trajectory (corresponding to 0 and 20 ns) are denoted by dashed arrows. The projected dynamics illustrate that the monomer is flexible and that it can adopt various structures beside the PDB structure (designated by a star). The various occupied regions of the 2D subspace are marked by ellipses, indicating that the bottom of the energy landscape of the monomer is rough and contains several basins connected by small barriers.

the two self-distance matrices, Δ_a and Δ_b.[66] The elements of the rectangular "cross" matrix are the distances between all conformations of molecule *a* and all conformations of molecule *b*. Thus, to obtain a joint projection of molecules *a* and *b*, PCA is applied to the combined matrix **D**,

$$\mathbf{D} = \begin{pmatrix} \Delta_a & \Delta_{a,b} \\ 0 & \Delta_b \end{pmatrix} \tag{5}$$

where Δ_a and Δ_b are the upper diagonal "self"-distance matrices and $\Delta_{a,b}$ is the rectangular "cross" distance matrix. The size of the joint **D** matrix is $(n + n') \times (n + n')$, with n conformations of molecule *a* and n' conformations of molecule *b*. Equation 5 is easily extended to any arbitrary number of analogous molecules.

In the present study, the PCA was applied to project the five conformational samples of either monomeric or dimeric HIV-1 PR onto the same subspace and in that way to explore the flexibility of each molecule and examine the region in conformational space sampled by each trajectory. Because each sample, obtained from a trajectory along 20 ns, contains 1000 conformations a 5000 × 5000 distance matrix **D** is calculated

$$\mathbf{D} = \begin{pmatrix} \Delta_{\text{trj1}} & \Delta_{\text{trj1,2}} & \Delta_{\text{trj1,3}} & \Delta_{\text{trj1,4}} & \Delta_{\text{trj1,5}} \\ 0 & \Delta_{\text{trj2}} & \Delta_{\text{trj2,3}} & \Delta_{\text{trj2,4}} & \Delta_{\text{trj2,5}} \\ 0 & 0 & \Delta_{\text{trj3}} & \Delta_{\text{trj3,4}} & \Delta_{\text{trj3,5}} \\ 0 & 0 & 0 & \Delta_{\text{trj4}} & \Delta_{\text{trj4,5}} \\ 0 & 0 & 0 & 0 & \Delta_{\text{trj5}} \end{pmatrix} \tag{6}$$

where the diagonal elements are the RMSD between the conformations generated by each simulation and the other nonzero elements are the RMSD between conformations generated by different simulations. In these calculations, the RMSD were calculated on the basis of the backbone without the flaps.

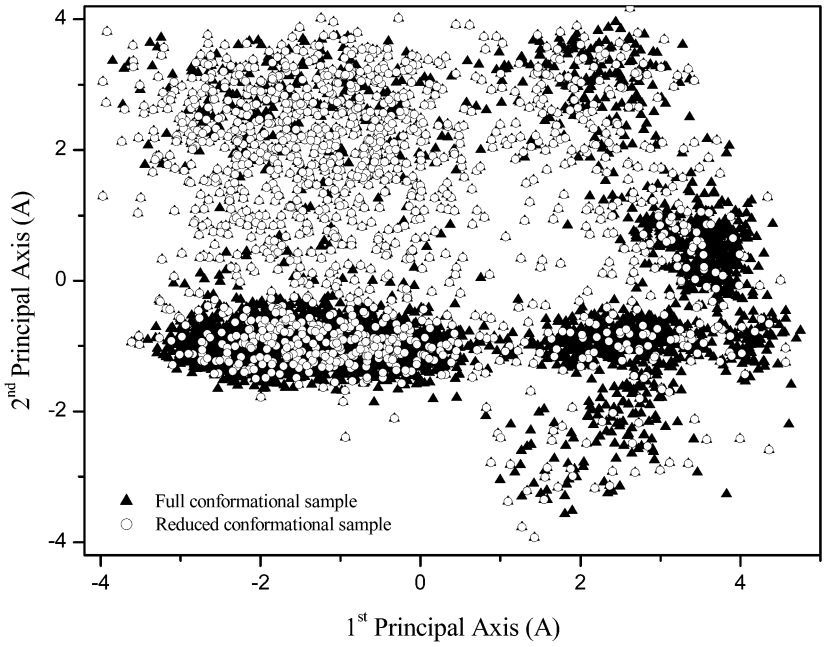

Figure 4. Principal coordinate projections of the full and reduced conformational samples of monomeric HIV-1 PR. The full sample includes 5000 conformations and is denoted by triangles and the reduced sample includes 1512 conformations and is denoted by circles.

Besides the comparison between the conformations generated by the five trajectories of the monomer and the dimer, the PCA is also used to examine the flexibility of the two identical subunits of the HIV-1 PR homodimer. To do so, the following 1210 × 1210 distance matrix is constructed

$$\mathbf{D} = \begin{pmatrix} \Delta_{\text{subunit } a} & \Delta_{\text{subunit } a,\text{subunit } b} \\ 0 & \Delta_{\text{subunit } b} \end{pmatrix} \tag{7}$$

where $\Delta_{\text{subunit } a}$ and $\Delta_{\text{subunit } b}$ are the "self"-distance matrix of subunit *a* and of subunit *b*, respectively, and $\Delta_{\text{subunit } a,\text{subunit } b}$ is the "cross" distance matrix between the conformations of subunit *a* and those of subunit *b*. Applying the PCA to this matrix may enable us to compare the flexibility of both subunits in the homodimeric structure.

To quantitatively explore the effect of the reduced flexibility due to dimerization, we compare the sampled conformational spaces of monomeric and dimeric HIV-1 protease. The calculation of this matrix is more difficult in comparison to the previous ones because comparing a monomeric conformation to a dimeric conformation is less intuitive as their chains are of different lengths (i.e., the monomer and the dimer composed of 99 and 198 residues, respectively). To overcome this limitation, the structural difference between a monomeric and a dimeric HIV-1 PR conformation was estimated by calculating the RMSD between the isolated monomer and each of the dimer subunits. To reduce the size of the matrix and make the calculations more efficient, each dimeric conformation is represented by one subunit. Moreover, among the two RMSD values, the largest was selected with the aim to represent the largest flexibility. This approach reflects the flexibility of the two subunits and ignores the inter-subunit motion. A similar approach was applied to quantify the flexibility of the dimeric isoform. In this case, the two subunits of a given conformation were compared with the two subunits of another dimeric conformation, resulting in four RMSD values. The maximal value among these four was selected to represent the largest structural variance of the dimeric HIV-1 PR. According to this scheme the following 2722 × 2722 distance matrix was calculated,

$$\mathbf{D} = \begin{pmatrix} \Delta_{\text{monomer}} & \Delta_{\text{monomer,dimer}} \\ 0 & \Delta_{\text{dimer}} \end{pmatrix} \tag{8}$$

where

$$\Delta_{\text{monomer,dimer}} = \max(\Delta_{\text{monomer,subunit}^i\ a}, \Delta_{\text{monomer,subunit}^i\ b}) \tag{9}$$

$$\mathbf{D}_{dimer} = \max\begin{pmatrix} \Delta_{\text{subunit}^i\ a,\text{subunit}^j\ a} & \Delta_{\text{subunit}^i\ b,\text{subunit}^j\ b} \\ \Delta_{\text{subunit}^i\ a,\text{subunit}^j\ b} & \Delta_{\text{subunit}^i\ b,\text{subunit}^j\ a} \end{pmatrix} \tag{10}$$

The 1512 × 1512 self-distance matrix Δ_{monomer} and the 1210 × 1210 self-distance matrix Δ_{dimer} represent the flexibility of the isolated monomer and the maximal flexibility of a single dimeric subunit (i.e., a bound monomer). The 1512 × 1210 cross-distance matrix $\Delta_{\text{monomer,dimer}}$ represents the difference in the flexibility of isolated and bound monomer.

All the 2D projections capture 40−52% of the normalized sum of all eigenvalues and the 3D projections capture 56−60% of that sum. The secondary structure determinations used for calculating the secondary structure content and for the preparation of Figure 10 were preformed by the program DSSP.[67]

Results and Discussion

Monomeric HIV-1 Protease. When the PCA is applied to the 5000 × 5000 monomeric HIV-1 PR distance matrix (eq 4), the whole conformational space of the protein as described by the 350 K trajectories can be characterized. Additionally, it is possible to examine the dynamics of the protein and evaluate its structural diversity. Figure 3 shows five projections (onto the same plane defined by the first two principal coordinates) of the conformations of monomeric HIV-1 PR sampled along the five 20 ns trajectories. The projections illustrate that the monomeric HIV-1 protease is flexible and adopts various structures that differ from the X-ray structure of the dimeric HIV-1 PR subunit. The maximal RMSD for the isolated monomer based on all backbone atoms without the flaps is 9.2

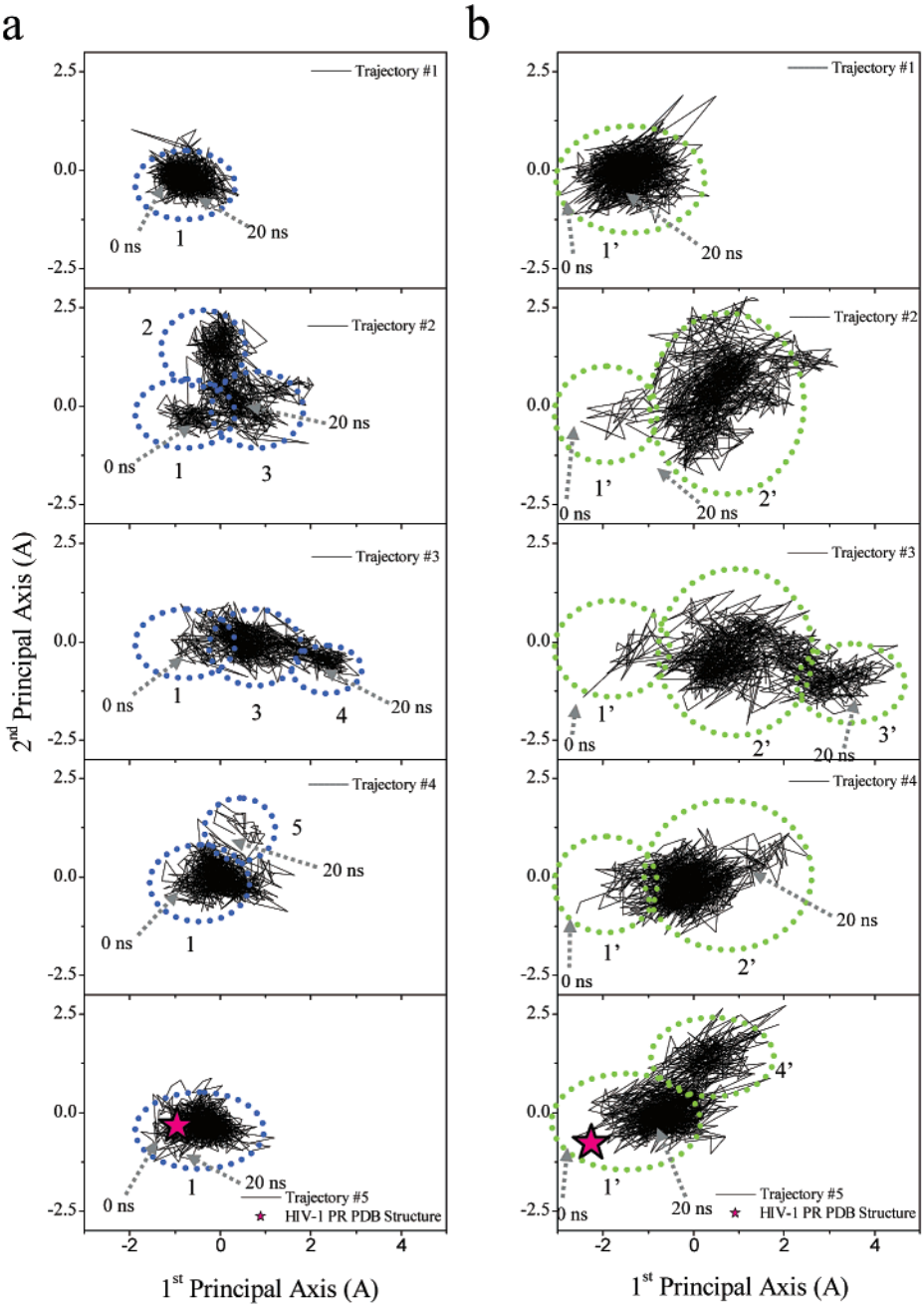

Figure 5. Projections of the five trajectories (simulated at 350 K) of dimeric HIV-1 PR onto a plane defined by the first two principal coordinates. The conformations are compared by calculating the RMS deviation based on the backbone atoms of a single subunit of the dimer (a) and based on all the backbone atoms of the two subunits (b). Whereas the projected trajectories in (a) illustrate the flexibility of a bound monomer, the projected trajectories in (b) include in addition the rigid body motion between the two bound subunits. Each trajectory includes 1000 conformations sampled along 20 ns. The initial and final sampled conformations in each trajectory (corresponding to 0 and 20 ns) are denoted by dashed arrows. The projected dynamics illustrates that the monomer is flexible and that it can adopt various structures besides the PDB structure (designated by a star). The various occupied regions of the 2D subspace are marked by ellipses, indicating that the bottom of the energy landscape of the dimer contains several basins, similar to that of the monomer (see Figure 3).

Å. Projecting a trajectory characterized by complex dynamics onto a plane defined by collective motions allows us to group the sampled conformations and to compare the initial and final structures to those sampled along the simulation. In the projected trajectories each group of conformations may correspond to a different basin on the energy landscape and is marked in Figure 3 by an ellipse. In the projection of trajectory #1 four regions are defined (regions 1−4). This indicates that the monomeric HIV-1 PR is flexible and can adopt other structures besides the structure of a single subunit of the symmetrical dimer. The projection of trajectory #2 indicates again the flexibility of the monomeric HIV-1 PR; however, in this trajectory only three groups of structures (regions 1, 3, and 5) are sampled. It is interesting to note that in trajectory #2 the monomeric HIV-1 PR visited two regions that were already detected by trajectory #1 (regions 1 and 3) and one additional region (region 5) is characterized. All other projected trajectories exhibit fluctuations between different conformational regions. The fact that seven regions, corresponding to different types of conformations, were sampled during a total of 100 ns may indicate that the bottom of the energy landscape of monomeric HIV-1 PR is rough and the transition between these basins is accessible at 350 K.

A single 20 ns trajectory at 350 K is not sufficient to represent the flexibility of the monomer. Accordingly, several trajectories

are required to characterize the conformational space of the flexible monomeric HIV-1 PR. However, the five trajectories include groups of similar conformations, which are redundant as far as mapping the conformational space is concerned. By applying a distance criterion, similar conformations are pruned from the conformational sample. Two conformations are defined as being similar if the backbone atom RMS between the two is smaller than 2 Å. After the redundant conformations are removed, the diluted sample includes 1511 conformations. To verify that the pruning does not affect the projections, the PCA was used to compare the conformation coverage before and after the reduction. Figure 4 shows the full and reduced conformational sample of the monomeric HIV and clearly indicates that the reduced conformational sample overlaps very well with the original full sample and that the reduction does not adversely affect the quality of the results.

Dimeric HIV-1 Protease. To explore the flexibility of the dimeric HIV-1 PR, its conformational space was sampled by applying a similar sampling procedure as for the monomeric HIV-1 PR, resulting in 5000 conformations. In three runs (trajectories #1, #4, and #5) the dimer was stable. The Cα RMSD oscillated around 2.2, 3.1, and 3.0 Å, respectively. In run2, the RMSD reached a value of about 5.5 Å in the first 4 ns and then decreased to about 3 Å. In run3, the structure deviated by about 3 Å until 12 ns, after which the RMSD increased to about 6 Å. To better explore the dimer flexibility and differences among the five trajectories, the multidimensional conformational space of the dimeric HIV-1 PR was projected onto 2D subspace obtained by the PCA. The motion of a dimeric protein consists of fluctuations within the two subunits and the relative reorientation between the two constituents. Accordingly, to study the dynamics of the dimeric HIV-1 PR, we define two RMSD measures for the flexibility of the dimer. In the first measure, the deviation between two dimeric conformations is calculated on the basis of a single subunit of the dimer (i.e., 99 residues) and thus reflects the internal flexibility of the bound monomer. In the second measure, the RMSD is calculated on the basis of all backbone atoms (i.e., 198 residues) and thus reflects both the internal flexibility of its two subunits and the relative motion between them. It should be noted that the distance matrices (eq 6) were calculated differently for the two RMSD measures. In the matrix calculated on the basis of the second RMSD, each element is the RMSD between pairs of dimeric conformations whereas in the corresponding matrix based on the first RMSD measure, each element is the largest RMSD among the four RMSDs calculated between the two subunits of one conformations and the two of another (similar to eq 10).

The dynamics of the bound monomeric HIV-1 PR at 350 K is characterized by sampling several conformational regions (Figure 5a). However, the dynamics of the bound monomeric HIV-1 PR (Figure 5b) is much reduced compared to that of the isolated monomer, as illustrated by the number of visited conformational regions and their structural diversity. The bound monomer samples five conformational regions compared to seven regions for the isolated monomer. Moreover, although the conformational regions of the isolated monomer include conformations with RMSD of about 9.2 Å (Figure 3), the maximal deviation described by the projected trajectories of the bound monomer is about 5.0 Å. The dynamics of the dimeric HIV-1 PR is more complicated than the dynamics of its moiety. Comparing the small area that is captured by the projected trajectories of the bound monomer (Figure 5a) to the relatively large area of the projected dimer trajectories (Figure 5b)

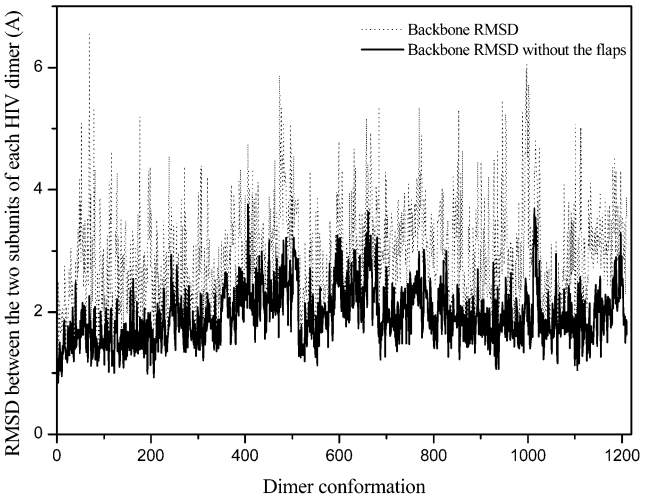

Figure 6. RMS deviation between the two subunits of each dimeric conformation (among the reduced sample) calculated on the basis of all backbone atoms (dashed line) and all backbone atoms without the flaps (black line).

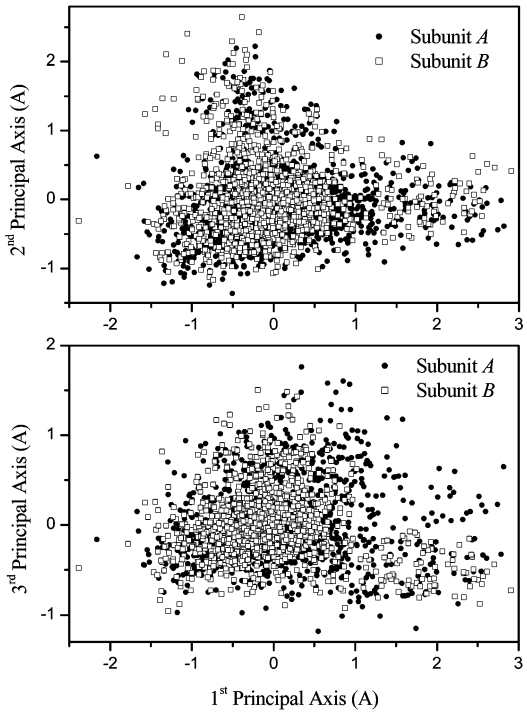

Figure 7. Joint projections of the sampled conformation spaces of the bound subunit A (full circles) and bound subunit B (empty circles) onto planes defined by the first and second principal axes (a) and by the first and third principal axes (b). The projections illustrate, as expected, that the flexibility of the two identical subunits of the HIV-1 PR is similar.

illustrates that the dimer experiences an additional relative motion between the two moieties. The dimer dynamics, as the dynamics of isolated and bound monomers, is characterized by traveling among different conformational regions (Figure 5b) where the maximal RMSD between any couple of conformations is 7.8 Å. The small RMSD values between the structures representing different conformational regions of the bound monomer suggests that, due to its reduced internal flexibility, extensive sampling by several trajectories is not required.

The full conformational sample of the dimeric HIV-1 PR was reduced from 5000 to 1210 conformations by applying a distance criterion of 1.8 Å cutoff. Because the HIV-1 PR dimer is composed of two identical subunits, it is interesting to explore

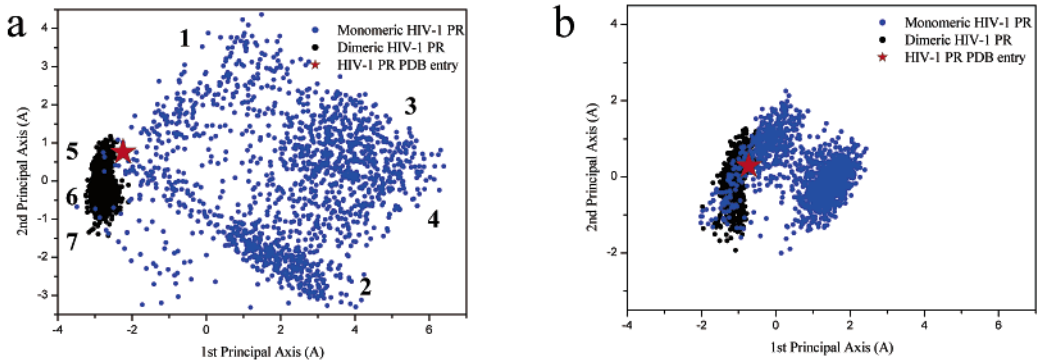

Figure 8. Joint projections of the monomeric and dimeric HIV-1 PR onto 2D subspace. The dimeric conformations are represented by one of its two subunits. The RMS deviation between the two conformations was calculated on the basis of all backbone atoms except for the flap (a) and on the basis of all backbone atoms except for the flap and the two terminals (b).

the flexibility of each subunit and to observe to what extent the complex remains symmetric along the trajectory. The RMSD between the two subunits of each dimeric HIV-1 PR conformation was calculated on the basis of the backbone atoms as well as on the backbone without the flaps (Figure 6). The average RMSD between the two moieties of the homodimer is about 1.9 Å and reflects that their dynamics is not symmetric. However, one may expect that because the two moieties of the dimer are identical, the volume of the conformational space covered by each of them should be the same.

To compare the flexibility of the two subunits, the PCA was applied on the distance matrix (eq 7). Figure 7 shows a joint projection of the 1210 conformations of subunit *A* as well as those of subunit *B* onto the best 2D subspace defined by the first two principal axes. As expected, the projected conformational spaces of the two identical subunits reflect similar flexibility. The fact that the two subunits of the dimeric HIV-1 PR sample similar regions indicates that the sampling covers the dimeric HIV-1 protease conformational space at 350 K. It is assumed that additional sampling at 350 K on a similar time scale may produce conformations that are similar to those that have been already sampled and would be redundant or "fill" holes in the joint 2D projection. Thus, additional conformations sampled along further 20 ns would not qualitatively affect the analysis.

Monomer Flexibility versus Dimer Flexibility. It is well-known, from both theoretical[23,25] and experimental[24,26] studies, that the flaps (residues 45−55) are flexible in both monomeric and dimeric forms of HIV-1 protease. Additionally, the N- and C-termini (residues 1−4 and 96−99, respectively) of the isolated monomer are flexible,[34] whereas in the dimer the termini constitute the interface between the two subunits and are therefore rigid.[41] Accordingly, two distance matrices (eq 8) were constructed: the first is based on the backbone atoms excluding the flap residues and the second on the backbone atoms excluding the flaps and the two termini. Figure 8 shows joint 2D projections of the monomeric and dimeric HIV-1 PR, as obtained by applying the PCA on the two isoforms of the distance matrix. The projected conformational space of the isolated monomeric protein is much larger than that of the dimeric protein and illustrates that the bound monomer is less flexible due to the interaction with the other subunit. Namely, the dimerization confines the structure of the monomer and the flexibility of each subunit is limited (Figure 8a). Neglecting the two termini results in larger overlap between the two conformational spaces (Figure 8b). Namely, the segments constituted of residues 5−44 and residues 56−95 of the monomeric and dimeric proteins have similar structures with larger flexibility

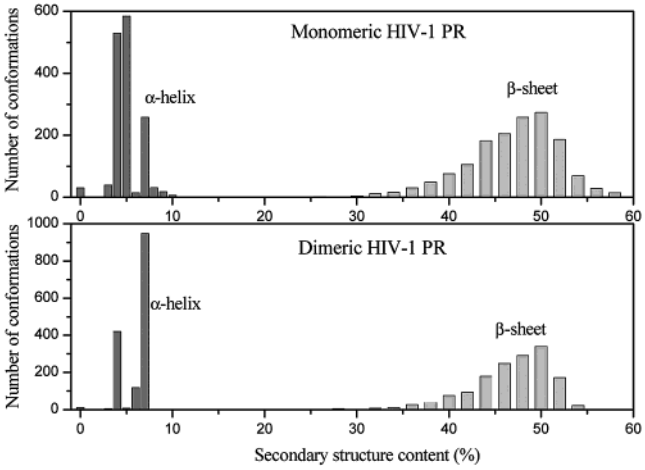

Figure 9. Histograms of the α-helical and *β*-sheet contents for monomeric and dimeric HIV-1 PR. The histograms indicate that the secondary structure contents of the isolated monomer and of the dimer are very similar. To focus on the monomer stability, the secondary structure of the dimeric structures were calculated for the subunits, thus neglecting the contribution of the interface. The calculations were done with the DSSP program.

for the isolated monomer. These projected conformational spaces demonstrate that the domain is quite stable in both monomeric and dimeric forms and most of the flexibility of the monomer is located in the two termini.

The N- and C-termini contribute most significantly to the subunit association, as reflected by their major contributions to the Gibbs energy of intersubunit interaction at the dimerization interface in comparison to other residues.[41] Accordingly, the large motion of the monomer in the interface region of HIV-1 PR is most likely due to solvation of residues that would be in close contact with the complementary subunit in the dimer. The loss of hydrophobic contacts, and *β*-sheet hydrogen bonds with the complementary subunit is the origin for the termini mobility when the other subunit is replaced by water. Similar flexibility of the termini of isolated monomeric HIV-1 PR were previously reported on the basis of 160 ps MD simulation at 300 K[35] and the general features of the tertiary structure were preserved over the course of that simulation.

To examine the stability of the domain of the monomeric and dimeric HIV-1 PR along the 100 ns MD simulations at 350 K, the secondary structure content of the conformational samples of both polypeptides was explored. Figure 9 shows histograms of the α-helical and *β*-sheet contents for both molecules. To focus on the monomer stability, the secondary structures of the dimeric structures were calculated for the

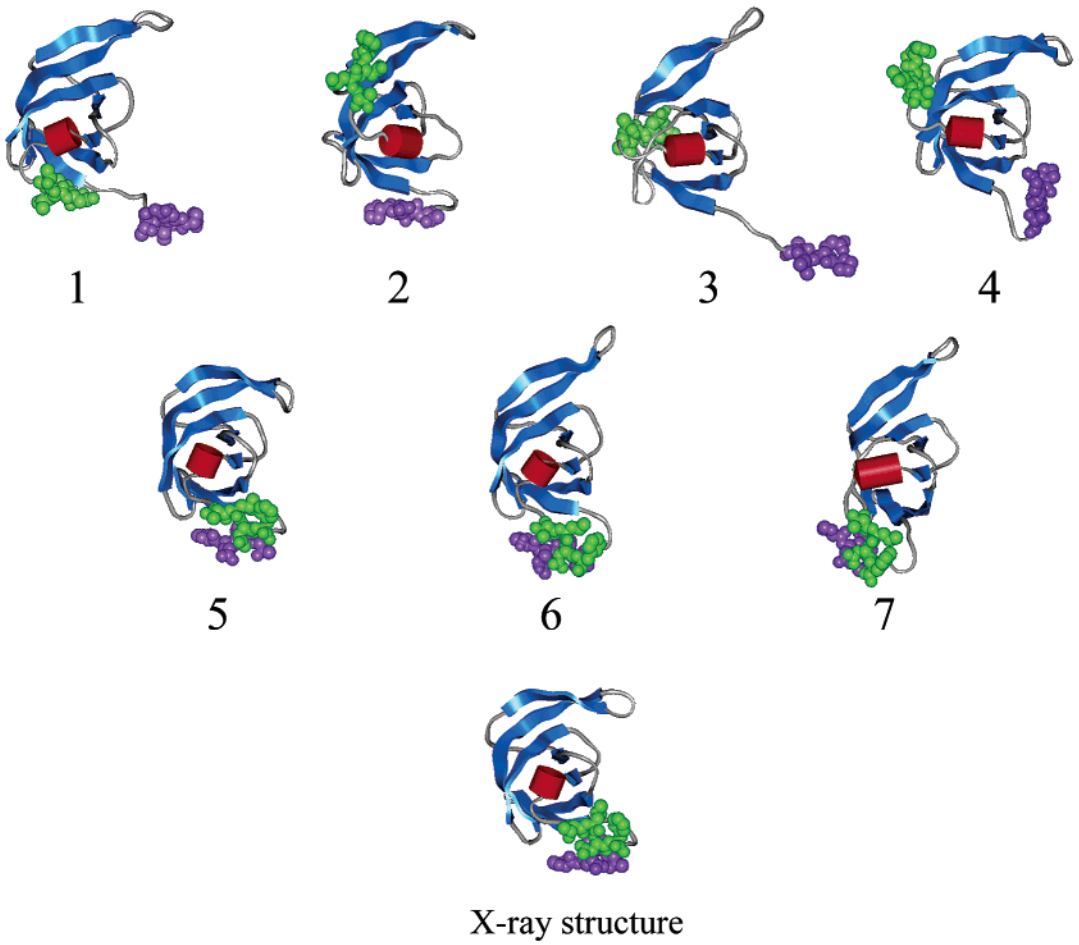

Figure 10. Four conformations of monomeric HIV-1 PR (conformations 1−4) and three conformations of the dimeric HIV-1 PR (conformations 5−7) selected from different regions of the projected conformation samples (Figure 8). For the dimeric HIV-1 PR only one subunit is shown. The β-sheets and α-helices are indicated in blue and red, respectively, and illustrate that the monomer is structured. The N- and C-termini are represented by green and purple vdW spheres to emphasize their destabilization and flexibility due to the absence of the second subunit. The secondary structure elements were determined on the basis of the DSSP program.

subunits, thus neglecting the four-stranded antiparallel β-sheet constituting the N- and C-termini of the monomers. The two histograms indicate that the secondary structure contents of the isolated monomer and of the dimer are very similar. This observation together with the fact that the monomer is more flexible than the dimer illustrates that the domain is stable and that the flexibility of the monomer is mainly of the termini and not due to the unfolding of secondary structure elements. Four monomeric conformations located at different regions of the joint 2D projection and three dimeric conformations were chosen to illustrate the stability of the secondary structure elements in both the monomer and dimer and the enhanced flexibility unique to the termini of the monomeric HIV-1 PR compared to their stability in the homodimeric protein (Figure 10). It should be noted that in the three dimeric structures only the subunit with the larger RMS deviation relative to the PDB structure is presented.

The conformations of the monomeric HIV-1 protease (Figure 10, top) and the conformations of the subunit of the dimeric HIV-1 protease (Figure 10, middle) illustrate that the secondary structure contents are very similar in each sample. The main structural difference between the monomeric and dimeric HIV-1 PR is related to the two termini. In the dimer, the two termini are close to each other and participate in the stabilizing interactions between the two subunits. In the monomer, due to the lack of interactions with the other subunit, the two termini are flexible. Additional evidence for the different flexibility of the two HIV-1 PR forms is obtained from the RMS fluctuations of each residue (Figure 11). This figure emphasizes that the flexibility of the monomer and dimer is very similar with the exception of the enhanced flexibility of the two termini of the monomer. Although the monomer is rather stable on the 20 ns time scale at 350 K, it is expected to unfold at longer time scales.

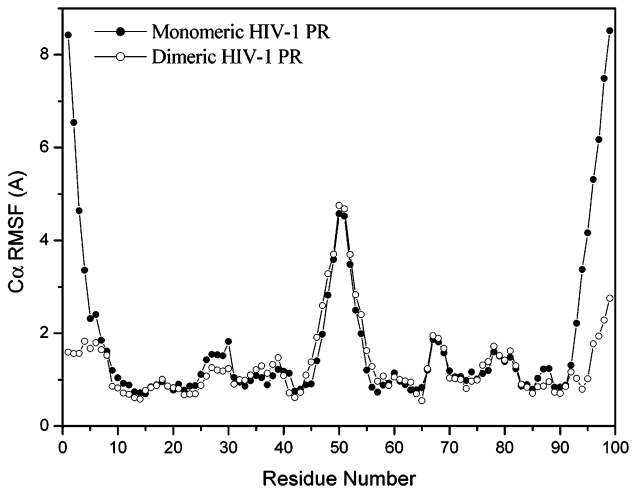

Figure 11. RMS fluctuations of the Cα atoms of monomeric and dimeric HIV-1 PR from the average 350 K conformation as a function of residue number.

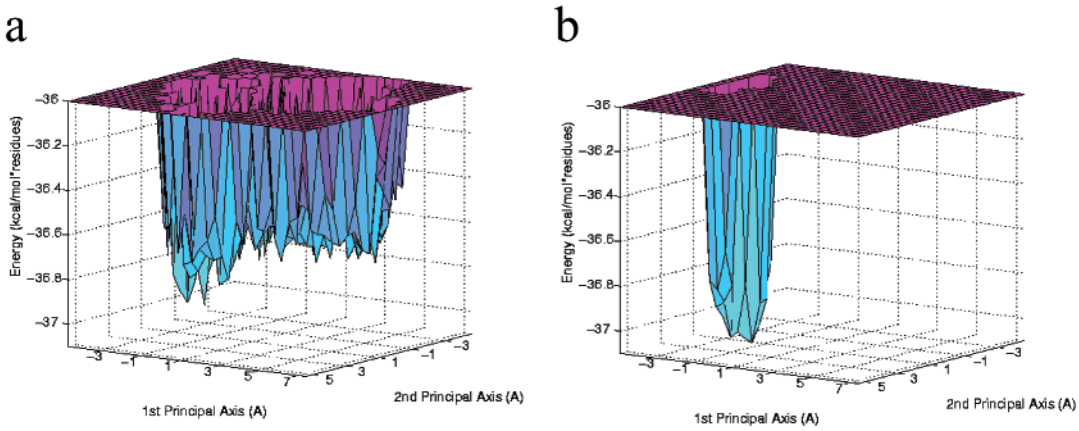

Figure 12. Energy landscapes of monomeric (a) and dimeric (b) HIV-1 PR. The *XY* plane represents the structural diversity of the monomeric and dimeric HIV-1 PR conformations as described in Figure 8a.

Energy Landscapes of Monomeric and Dimeric HIV-1 Protease. The different dynamic properties of the monomeric and dimeric HIV-1 PR are a consequence of their energy landscapes. To highlight the topography of the energy landscape the "minimal energy envelope" was applied by adding the potential energy of each conformation to the 2D projected conformational spaces.[61] Using this approach, the effect of conformational constraints,[66,68] the solvent,[55] and point mutations[65] on the energy landscapes of polypeptides were studied. Because the conformational space of the dimer is characterized by one of its two subunits, the potential energy of a dimeric conformation was divided by 2. The potential energy is interpreted in terms of stability, and the joint projected conformational space of the monomer and dimer (Figure 8) enables us also to compare *structural diversity*. Because in the present study the conformations were sampled with moderately high temperature MD simulations (350 K), crossing high barriers is impossible and thus only thermodynamically and kinetically stable conformations were sampled. Accordingly, only the bottom of the energy landscape is described.

Figure 12 shows the bottom of the energy landscapes of monomeric (Figure 12a) and dimeric (Figure 12b) HIV-1 PR. The topography of the two energy landscapes is significantly different, reflecting the different dynamics of the two proteins. The energy landscape of monomeric HIV-1 PR is broad and contains multiple local minima whereas the energy landscape of the dimer is narrower and deeper. These properties are reflected in the high flexibility of the isolated monomer and the small structural fluctuations of the dimer. Moreover, the global minimum of the dimeric HIV-1 PR is deeper, indicating larger stability, presumably due to the hydrophobic interaction between the two subunits. Recently, a statistical survey of crystal structures with different inhibitors complemented by MD simulations and normal modes analysis was published. The authors suggested that the potential energy surface of the HIV-1 PR is characterized by many local minima in the neighborhood of the native state that differ little in energy.[40] This is in agreement with our results as reflected by the flexibility of the dimer (Figure 5). We also propose that the flexibility of the monomer is larger than that of the dimer and the bottom of its energy landscape is rougher.

The energy landscapes of monomeric and dimeric HIV-1 PR illustrate the effect of association on the dynamics and on the stability. Although the energy landscape of an isolated subunit is rough and shallow, the energy landscape of a bound subunit is smoother and deeper. The properties of the energy landscape of a dimeric protein, as found in the present study, are in good agreement with a prediction made by Nussinov and her colleagues on the effects of binding and association on an energy landscape of an isolated protein. They suggest that if a dimer is formed by association of two already folded proteins (i.e., a three-state dimer), the funnel landscape of the complex can be considered as the fusing of two individual folding funnels of the monomers, making the bottom of the newly fused funnel deeper and occupied by a collection of favorable associations of two conformations.[69,70] It should be noted that because only the bottom of the dimer energy landscape is presented here, only conformations that are stabilized by the termini swapping are described and thus the focus is on the stability and flexibility of the formed dimer. To study the mechanism of termini swapping, upper regions of the landscape have to be explored.

Conclusions

The flexibility of monomeric and dimeric forms of HIV-1 protease was studied by MD simulations. The sampled conformations were projected on a two-dimensional subspace whose axes were obtained by applying the principal component analysis (PCA) on the distance matrix of each molecule. In agreement with NMR measurements[24,26] and previous MD simulations,[23,25] it was found that the flap tips (residues 45−55) are flexible and adopt closed and completely open conformations in solution. The isolated monomeric HIV-1 PR is more flexible than the dimeric HIV-1 PR. The projected trajectories illustrate that the monomer adopts various conformations, which are grouped using the collective coordinates into seven clusters where the maximal RMSD among the 5000 projected conformations is 9.2 Å. The limited dynamics of each of the two subunits that constitute the dimeric HIV-1 PR is reflected by only three visited conformational regions that have a maximal RMSD of about 5.0 Å. It was found that although the dynamics of the dimer is not symmetric (the average RMS deviation between the two identical subunits of a given dimeric conformation is 1.9 Å), the flexibility of the two subunits is identical and they sample similar regions of conformational space. The motion of the dimer has two important components: the first is an intradynamics of each of the subunits and the second is the displacement of one subunit with respect to the other. Though the intradynamics is very significant for the isolated monomer, it is minor for the dimer. The interaction between the two subunits constrains their internal flexibility and the major contribution to the dynamics of the dimer, besides the flap motion, is the relative motion between the two bound monomers.

The different flexibility of the isolated and bound monomer is reflected in the topography of its underlying energy land-

scapes. The bottom of the dimer energy landscape is deeper and much narrower than the one of the monomer. Moreover, the energy landscape of the isolated monomer is rougher (i.e., contains multiple minima) than that of the dimer, reflecting its enhanced flexibility. The fact that the energy landscape of the bound monomer is deeper in comparison to that of the isolated monomer illustrates that the interactions between the two subunits at the interface stabilize each subunit. The enhanced flexibility of the isolated monomer is mostly in the N- and C-termini (residues 1−4 and 96−99, respectively), which are almost rigid in the dimeric form. This observation suggests, in agreement with a previous study,[41] that the two termini constitute the interface between the two subunits and contribute significantly to subunit association, indicating that blocking one (or both) of them may prevent the formation of the active enzyme.

With the exception of the different flexibility of the N- and C-termini, the tertiary structure of the two HIV-1 PR forms is very similar and no destabilization of secondary structure elements was observed. This result suggests that along 20 ns trajectories at neutral pH and 350 K the monomer is structured; however, it is expected to unfold at longer time scales. It should be noted that under denaturating conditions (i.e., denaturant, high temperature, or low pH) the monomeric form of HIV-1 PR is unstable and the dimer unfolding was described by a two-state model in which folded dimers were in equilibrium with unfolded monomers.[12,41] In addition, the dissociation of the dimeric HIV-1 PR under physiological conditions is accompanied by a loss of β-sheet content,[39] which may be attributed to the breaking up of the four-stranded antiparallel β-sheets that define the interface between the two subunits, whereas the monomers remained structured. NMR measurements on a mutant protease containing the R87K substitution showed that the monomer is folded with a structure similar to a single subunit of the dimer.[34]

The finding that the isolated monomeric HIV-1 PR has similar secondary and tertiary structure as a single subunit of the dimer suggests that under physiological conditions the active dimer is in equilibrium with a partially structured monomer. Moreover, the existence of structured monomer suggests that partial folding of the monomer is a prerequisite for the dimerization of the HIV-1 PR and thus the folding and recognition are not coupled processes, indicating that the folding of dimeric HIV-1 PR may not obey a two-state model. On the basis of the flexibility of the monomer termini and the fact that they constitute the interface between the two subunits, we propose that the association of the HIV-1 PR subunits follows a domain swapping mechanism, which involves the exchange of the flexible termini across the two chains as illustrated in Figure 1b. Additional support for the description of the association of HIV-1 PR by domain swapping was previously obtained from the compactness profile of the dimer, which resembles that of known domain-swapped dimers rather than that of known two-state dimers.[7]

Categorizing the HIV-1 PR as a two-state dimer based on equilibrium denaturation experiments might be explained by the low value of K_d (50 nM and 0.023 nM at pH = 3.4 and 5.0, respectively)[41] and by the fact that these experiments were performed at significantly higher concentrations (few micromolar) than that in vivo, as dictated by the instrument sensitivity. Because the unfolding of a three-state dimer is concentration dependent, experiments should be carried out at a lower concentrations (i.e., values similar to that of the K_d) to asses the validity of a two- or three-state dimerization model.[71] At concentration much larger than the dimer's K_d a monomeric intermediate becomes unstable relative to the dimer and therefore is less populated at equilibrium. Accordingly, the dimer might be wrongly classified as a two-state dimer. Presumably, folded monomeric HIV-1 PR R87K mutant was detected because of the loss of specific interactions at the interface.[34] Destabilization of the dimer by the mutation results in higher K_d and enables detection of the folded monomer even at concentrations of a few micromolar. On the basis of MD simulations, we propose that wild-type HIV-1 PR is a three-state dimer and expect that more sensitive instrumentation will be able to detect a folded monomeric HIV-1 PR.

Acknowledgment. We are very grateful to Ruth Nussinov for stimulating discussions and for critical reading of the manuscript. We thank John M. Louis for illuminating discussion. We also thank Leslie Chavez for critical reading of the manuscript and Urs Haberthus and Jörg Gsponer for their help with CHARMM. Y.L. thanks the Clore foundation for support. This work was partially supported by the Swiss National Competence Center in Structural Biology (NCCR).

References and Notes

(1) Goodsell, D. S.; Olson, A. J. *Annu. Rev. Biophys. Biomol. Struct.* **2000**, *29*, 105−153.
(2) Blundell, T. L.; Srinivasan, N. *Proc. Natl. Acad. Sci. U.S.A.* **1996**, *93*, 14243−14248.
(3) Wolynes, P. G. *Proc. Natl. Acad. Sci. U.S.A.* **1996**, *93*, 14249−14255.
(4) Dobson, C. M. *Trends Biochem. Sci.* **1999**, *24*, 329−332.
(5) Soto, C. *FEBS Lett.* **2001**, *498*, 204−207.
(6) Katzir, E.; Solomon, B.; Taraboulos, A. In *Conformational Diseases*; Bialik: Jerusalem, 2001.
(7) Xu, D.; Tsai, C.-J.; Nussinov, R. *Protein Sci.* **1998**, *7*, 533−544.
(8) D'Alessio, G. *Prog. Biophys. Mol. Biol.* **1999**, *72*, 271−298.
(9) Seckler, R. *Assembly of multi-subunit structures. In Mechanisms of protein folding*. 2nd ed.; Oxford University Press: Oxford, U.K., 2000.
(10) Bowie, J. U.; Sauer, R. T. *Biochemistry* **1989**, *28*, 7139−7143.
(11) Gittelman, M. S.; Matthews, C. R. *Biochemistry* **1990**, *29*, 7011−7020.
(12) Grant, S. K.; Deckman, I. C.; Culp, J. S.; Minnich, M. D.; Brooks, I. S.; Hensley, P.; Debouck, C.; Meek, T. D. *Biochemistry* **1992**, *31*, 9491−9501.
(13) Neet, K. E.; Timm, D. E. *Protein Sci.* **1994**, *3*, 2167−2174.
(14) Bennett, M. J.; Schlunegger, M. P.; Eisenberg, D. *Protein Sci.* **1995**, *4*, 2455−2468.
(15) Liu, Y.; Eisenberg, D. *Protein Sci.* **2002**, *11*, 1285−1299.
(16) Newcomer, M. E. *Curr. Opin. Struct. Biol.* **2002**, *12*, 48−53.
(17) Dunker, A. K.; Lawson, J. D.; Brown, C. J.; Williams, R. M.; Romero, P.; Oh, J. S.; Oldfield, C. J.; Campen, A. M.; Ratliff, C. M.; Hipps, K. W.; Ausio, J.; Nissen, M. S.; Reeves, R.; Kang, C.; Kissinger, C. R.; Bailey, R. W.; Griswold, M. D.; Chiu, W.; Garner, E. C.; Obradovic, Z. *Journal of Mol. Graphics Modelling* **2001**, *19*, 26−59.
(18) Dyson, H. J.; Wright, P. E. *Curr. Opin. Struct. Biol.* **2002**, *12*, 54−60.
(19) Uversky, V. N. *Eur. J. Biochem.* **2002**, *269*, 2−12.
(20) Wlodawer, A.; Miller, M.; Jaskolski, M.; Sathyanarayana, B. K.; Baldwin, E.; Weber, I. T.; Selk, L. M.; Clawson, L.; Schneider, J.; Kent, S. B. H. *Science* **1989**, *245*, 616−621.
(21) Lapatto, R.; Blundell, T.; Hemmings, A.; Overington, J.; Wilderspin, A.; Wood, S.; Merson, J. R.; Whittle, P. J.; Danley, D. E.; Geoghegan, K. F.; Al, E. *Nature* **1989**, *342*, 299−302.
(22) Nicholson, L. K.; Yamazaki, T.; Torchia, D. A.; Grzesiek, S.; Bax, A.; Stahl, S. J.; Kaufman, J. D.; Wingfield, P. T.; Lam, P. Y. S.; Jadhav, P. K.; Hodge, C. N.; Domaille, P. J.; Chang, C.-H. *Struct. Biol.* **1995**, *2*, 274−280.
(23) Rick, S. W.; Erickson, J. W.; Burt, S. K. *Proteins Struct. Funct. Genet.* **1998**, *32*, 7−16.
(24) Ishima, R.; Freedberg, D. I.; Wang, Y.-X.; Louis, J. M.; Torchia, D. A. *Structure* **1999**, *7*, 1047−1055.
(25) Scott, W. R. P.; Schiffer, C. A. *Structure* **2000**, *8*, 1259−1265.
(26) Freedberg, D. I.; Ishima, R.; Jacob, J.; Wang, Y.-X.; Kustanovich, I.; Louis, J. M.; Torchia, D. A. *Protein Sci.* **2002**, *11*, 221−232.
(27) Debouck, C. *AIDS Res. Hum. Retroviruses* **1992**, *8*, 153−164.
(28) Huff, J. R. *J. Med. Chem.* **1991**, *34*, 2305−2314.
(29) Fitzgerald, P. M. D.; Spirnger, J. P. *Annu. Rev. Biophys. Chem.* **1991**, *20*, 299−320.

(30) Blundell, T. L.; Lapatto, R.; Wilderspin, A. F.; Hemmings, A. M.; Hobart, P. M.; Danley, D. E.; Whittle, P. J. *Trends. Biochem. Sci.* **1990**, *15*, 425−430.
(31) Zutshi, R.; Franciskovich, J.; Shultz, M.; Schweitzer, B.; Bishop, P.; Wilson, M.; Chmielewski, J. *J. Am. Chem. Soc.* **1997**, *119*, 4841−4845.
(32) Zutshi, R.; Chmielewski, J. *Bioorg. Med. Chem.* **2000**, *10*, 1901−1903.
(33) Caflisch, A.; Schramm, H. J.; Karplus, M. *J. Comput.-Aided Mol. Design* **2000**, *14*, 161−179.
(34) Ishima, R.; Ghirlando, R.; Tozser, J.; Gronenborn, A. M.; Torchia, D. A.; Louis, J. M. *J. Biol. Chem.* **2001**, *276*, 49110−49116.
(35) Venable, R. M.; Brooks, B. R.; Carson, F. W. *Proteins Struct. Funct. Genet.* **1993**, *15*, 374−384.
(36) Swaminathan, S.; Harte, W. E., Jr.; Beveridge, D. L. *J. Am. Chem. Soc.* **1991**, *113*, 2717−2721.
(37) York, D. M.; Darden, T. A.; Pedersen, L. G.; Anderson, M. W. *Biochemistry* **1993**, *32*, 1443−1453.
(38) Collins, J. R.; Burt, S. K.; Erickson, J. W. *Struct. Biol.* **1995**, *2*, 334−338.
(39) Thrope, M. F.; Lei, M.; Rader, A. J.; Jacob, D. J.; Kuhn, L. A. *J. Mol. Graphics Modelling* **2001**, *19*, 60−69.
(40) Zoete, V.; Michielin, O.; Karplus, M. *J. Mol. Biol.* **2002**, *315*, 21−52.
(41) Todd, M. J.; Semo, N.; Freire, E. *J. Mol. Biol.* **1998**, *283*, 475−488.
(42) Xie, D.; Gulnik, S.; Gusrchina, E.; Yu, B.; Shao, W.; Qoronfleh, W.; Nathan, A.; Erickson, J. W. *Protein Sci.* **1999**, *8*, 1702−1707.
(43) Spinelli, S.; Liu, Q. Z.; Alzari, P. M.; Hirel, P. H.; Poljak, R. J. *Biochimie* **1991**, *73*, 1391−1396.
(44) Brooks, B. R.; Bruccoleri, R. E.; Olafson, B. D.; States, D. J.; Swaminathan, S.; Karplus, M. *J. Comput. Chem.* **1983**, *4*, 187−217.
(45) Lazaridis, T.; Karplus, M. *Proteins Struct. Funct. Genet.* **1999**, *35*, 133−152.
(46) Dinner, A.; Lazaridis, T.; Karplus, M. *Proc. Natl. Acad. Sci. U.S.A.* **1999**, *96*, 9068−9073.
(47) Kumar, S.; Sham, Y.; Tsai, C.-J.; Nussinov, R. *Biophys. J.* **2001**, *80*, 2439−2454.
(48) Tsai, C.-J.; Ma, B.; Sham, Y.; Kumar, S.; Nussinov, R. *Proteins Struct. Funct. Genet.* **2001**, *44*, 418−427.
(49) Paci, E.; Karplus, M. *J. Mol. Biol.* **1999**, *288*, 441−449.
(50) Inuzuka, Y.; Lazaridis, T. *Proteins Struct. Funct. Genet.* **2000**, *41*, 21−32.
(51) Lazaridis, T.; Karplus, M. *J. Mol. Biol.* **1999**, *288*, 477−487.
(52) Lazaridis, T.; Karplus, M. *Curr. Opin. Struct. Biol.* **2000**, *10*, 139−145.
(53) Petrella, R.; Karplus, M. *J. Phys. Chem. B* **2000**, *104*, 11370−11378.
(54) Lazaridis, T.; Karplus, M. *Science* **1997**, *278*, 1928−1931.
(55) Levy, Y.; Jortner, J.; Becker, O. M. *Proc. Natl. Acad. Sci. U.S.A.* **2001**, *98*, 2188−2193.
(56) Levy, Y.; Hanan, E.; Solomon, B.; Becker, O. M. *Proteins Struct. Funct. Genet.* **2001**, *45*, 382−396.
(57) Kitao, A.; Go, N. *J. Comput. Chem.* **1991**, *12*, 359.
(58) Garcia, A. E. *Phys. Rev. Lett.* **1992**, *68*, 2696.
(59) Garcia, A. E.; Herman, J. G. *Protein Sci.* **1996**, *5*, 62.
(60) Amadei, A.; Linssen, A. B. M.; Berendsen, H. J. C. *Proteins Struct. Funct. Genet.* **1993**, *17*, 412.
(61) Becker, O. M. *J. Comput. Chem.* **1998**, *19*, 1255−1267.
(62) Kitao, A.; Go, N. *Curr. Opin. Struct. Biol.* **1999**, *9*, 164−169.
(63) Hayward, S.; Go, N. *Annu. Rev. Phys. Chem.* **1995**, *46*, 223−250.
(64) Becker, O. M.; Levy, Y.; Ravitz, O. *J. Phys. Chem. B* **2000**, *104*, 2123−2135.
(65) Levy, Y.; Becker, O. M. *Proteins Struct. Funct. Genet.* **2002**, *47*, 458−468.
(66) Levy, Y.; Becker, O. M. *J. Chem. Phys.* **2001**, *114*, 993−1009.
(67) Kabsch, W.; Sander, C. *Biopolymers* **1983**, *22*, 2577−2637.
(68) Levy, Y.; Jortner, J.; Becker, O. M. *J. Chem. Phys.* **2001**, *115*, 10533−10547.
(69) Ma, B.; Kumar, S.; Tsai, C.-J.; Nussinov, R. *Protein Eng.* **1999**, *12*, 713−720.
(70) Tsai, C.-J.; Kumar, S.; Ma, B.; Nussinov, R. *Protein Sci.* **1999**, *8*, 1181−1190.
(71) Hobart, S. A.; Ilin, S.; Moriarty, D. F.; Osuna, R.; Colon, W. *Protein Sci.* **2002**, *11*, 1671−1680.